

Interleavers and BCH Codes for Coherent DQPSK Systems with Laser Phase Noise

Miu Yoong Leong, Knud J. Larsen, Gunnar Jacobsen, Sergei Popov, Darko Zibar, and Sergey Sergeyev

Abstract—The relatively high phase noise of coherent optical systems poses unique challenges for forward error correction (FEC). In this letter, we propose a novel semi-analytical method for selecting combinations of interleaver lengths and binary Bose-Chaudhuri-Hocquenghem (BCH) codes that meet a target post-FEC bit error rate (BER). Our method requires only short pre-FEC simulations, based on which we design interleavers and codes analytically. It is applicable to pre-FEC BER around 10^{-3} , and any post-FEC BER. Additionally, we show that there is a trade-off between code overhead and interleaver delay. Finally, for a target of 10^{-5} , numerical simulations show that interleaver-code combinations selected using our method have post-FEC BER around $2\times$ target. The target BER is achieved with 0.1 dB extra signal-to-noise ratio.

Index Terms—Optical fiber communications, error correction codes, block codes, phase noise, communication systems.

I. INTRODUCTION

FORWARD error correction (FEC) is crucial for coherent optical systems with multi-level modulation. Traditionally, coding theory focuses on additive white Gaussian noise (AWGN) channels with independent identically distributed (i.i.d.) errors [1]–[3]. However, some communication systems have non-i.i.d. errors. This affects the choice of FEC codes. For example, wireless systems use codes that correct burst errors from fading. In the case of coherent optical systems, transmitter and local oscillator (LO) lasers have relatively high phase noise (PN). Algorithms for estimating and compensating PN result in non-zero probability of cycle slips [4], [5]. We consider codes specifically for such systems. Recently, several approaches have been proposed. In [6]–[8], the authors consider low-density parity-check (LDPC) codes. In [9], we consider binary Bose-Chaudhuri-Hocquenghem (BCH) and Reed-Solomon (RS) codes. In [10], we improve the method for dimensioning binary BCH codes in [9] by using a bivariate distribution. However, the codes selected using the method in [10] have high overhead, which reduces system throughput.

In this letter, we propose to use interleaving to reduce code overhead, by trading it off with interleaver delay. In systems that can tolerate the additional processing delay, we

can achieve higher throughputs compared to [10]. Specifically, this letter has three significant contributions. First, we propose a novel method for determining combinations of binary BCH codes and interleaver lengths that achieve a target post-FEC bit error rate (BER). Our method includes the method in [10] as the special case of no interleaving. Second, we establish that a trade-off exists between code overhead and interleaver delay. Third, we present numerical simulations to verify the accuracy of our method. Ours is a straightforward method, based on a simple model, that enables us to design low-complexity interleavers and binary BCH codes for any post-FEC BER with little simulation effort. Compared to our method, the approaches presented in [6]–[8] achieve better performance by using soft information. However, those schemes are more complex to implement, and require extensive simulations for low post-FEC BERs.

This letter is organized as follows: the system model and interleaver-and-code selection are described in Sec. II. Simulation results and discussion are in Sec. III. The trade-off between code overhead and interleaver delay is discussed in Sec. III-A. Post-FEC simulations are presented in Sec. III-B. Finally, the conclusion is in Sec. IV.

II. INTERLEAVER AND CODE SELECTION

We add interleaving to [10], resulting in the baseband-equivalent system in Fig. 1. A (possibly shortened) binary BCH code $\text{BCH}(n_{B,S}, k_{B,S})$ corrects up to at least τ bit errors [3], [10]. The code has block length $n_{B,S}$ bits, of which $k_{B,S}$ are data bits. In the transmitter, we use a block interleaver of length L code blocks. The interleaver reorders the $L \cdot n_{B,S}$ bits within those code blocks using a known input-output mapping. In the receiver, the deinterleaver applies the opposite mapping, thereby returning the bits to their original order. The interleaver mapping is generated by a pseudorandom sequence, but this may occasionally result in an interleaver with inferior performance for specific error patterns. By generating the mapping randomly for each interleaver frame, we approximate the performance over the ensemble of interleavers and it is expected that this will be representative of the performance of a well-chosen interleaver. This is of course not practical for implementation so some care must be taken in selecting the interleaver.

Without interleaving, bit errors are correlated so code blocks with errors tend to have many errors [10]. To correct these errors, stronger codes with higher overheads are needed. With interleaving, the deinterleaver redistributes the errors. The idea is to decorrelate and spread errors more evenly across

M.Y. Leong and G. Jacobsen are with Acreo Swedish ICT, Box 1070, 16425 Stockholm, Sweden and KTH Royal Institute of Technology, 16440 Stockholm, Sweden e-mail: miuyoong.leong@acreo.se.

K.J. Larsen and D. Zibar are with the Technical University of Denmark (DTU), 2800 Kgs. Lyngby, Denmark.

S. Popov is with KTH Royal Institute of Technology, Stockholm, Sweden.

S. Sergeyev is with Aston University, Birmingham, United Kingdom.

Manuscript received September 26, 2014; revised [TBD: date], 2014; accepted [TBD: date], 2014. Date of publication [TBD: date], 2014; date of current version [TBD: date], 2014.

Digital Object Identifier [TBD: TBD]

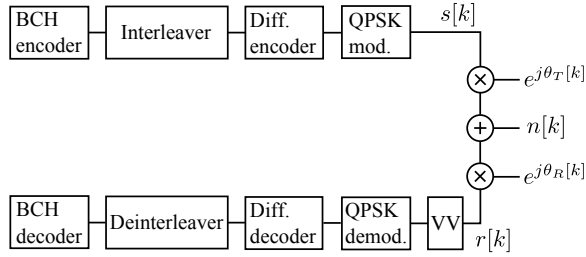


Fig. 1. System model. A random bit sequence is BCH encoded, interleaved, differentially encoded, and Quadrature Phase Shift Keying (QPSK) modulated. This yields signal $s[k]$. Channel impairments are transmitter laser PN $\theta_T[k]$, AWGN $n[k]$, and LO laser PN $\theta_R[k]$. Phase estimation on the received signal $r[k]$ is by Viterbi-Viterbi (VV). Finally, the signal is QPSK demodulated, differentially decoded, deinterleaved, and BCH decoded.

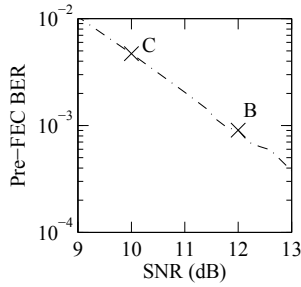


Fig. 2. Poor phase estimate (PE), pre-FEC BER. We design interleaver-and-code combinations for “poor PE pre-FEC” points C (SNR 10 dB) and B (SNR 12 dB). The SNR is for symbols $r[k]$ in Fig. 1.

code blocks. This allows us to use weaker codes with lower overheads. However, interleaving adds delay as bits must be collected before remapping in the interleaver and deinterleaver. The delay is proportional to interleaver length L .

We want to find combinations of interleaver length L and code error correcting capability τ that achieve a target post-FEC BER with code block length $n_{B,S}$. To do so, we first obtain a statistical model of the system without interleaving using the method in [10]. Namely, for a given laser linewidth-symbol time product, we optimize the length of the Viterbi-Viterbi (VV) moving average filter using pre-FEC simulations. Then, for the linewidth variations that we want to accommodate, we simulate a worst-case “poor phase estimate (PE)” curve (Fig. 2). As described in [10], for a point on this curve, we record its error statistics and use them to parameterize a correlated bivariate binomial probability density function (PDF) $\Pr(Y_G = y_G, Y_C = y_C)$. The random variable Y_G represents the number of AWGN error patterns $\{0110, 1010, 0101, 1001\}$ in a code block of $n_{B,S}$ bits. The random variable Y_C represents the number of cycle slips (single bit errors) in a code block. We neglect 180° errors as these have very low probabilities. The correlation between Y_G and Y_C is due to VV phase estimation [10], and depends on the operating point e.g. signal-to-noise ratio (SNR), laser linewidths, and filter length. This bivariate model is specific to coherently-demodulated Differential Quadrature Phase Shift Keying (DQPSK) systems using VV phase estimation.

The rest of this section describes our novel method for determining suitable interleaver-code combinations. We collapse

the two-dimensional joint PDF $\Pr(Y_G = y_G, Y_C = y_C)$ into a one-dimensional PDF $\Pr(Y_A = y_A)$. The random variable Y_A represents the total number of bit errors in a code block, including both AWGN errors and cycle slips

$$\Pr(Y_A = y_A) = \sum_{(y_G, y_C): 2y_G + y_C = y_A} \Pr(Y_G = y_G, Y_C = y_C). \quad (1)$$

A factor of 2 multiplies y_G because AWGN error patterns have two bit errors.

Let Y_L be a random variable representing the total number of bit errors in L code blocks. The PDF of Y_L is the L -fold convolution of $\Pr(Y_A = y_A)$ with itself

$$\begin{aligned} \Pr(Y_L = y_L) &= \Pr(Y_A = y_A)^{\star L} \\ &= \sum_{(y_{A,1}, y_{A,2}, \dots, y_{A,L}) \in \Psi} \Pr(Y_A = y_{A,1}) \times \\ &\quad \Pr(Y_A = y_{A,2}) \times \dots \times \Pr(Y_A = y_{A,L}) \end{aligned} \quad (2)$$

where Ψ is the set of $(y_{A,1}, y_{A,2}, \dots, y_{A,L})$ such that $y_{A,1} + y_{A,2} + \dots + y_{A,L} = y_L$, and $L \in \{1, 2, 3, \dots\}$. For $L = 1$, $\Pr(Y_L = \xi) = \Pr(Y_A = \xi)$, i.e. in this case $y_L = y_A = \xi$. For $L = 2$, $\Pr(Y_L = y_L) = \Pr(Y_A = y_A) \star \Pr(Y_A = y_A)$. Convolution is denoted by \star . We neglect edge effects in the convolution, as the probability of an AWGN error starting on the last symbol of a code block is small for pre-FEC BER of 10^{-3} and typical code block lengths (cf. Table I).

Deinterleaving distributes the y_L bit errors over L code blocks. This is analogous to the balls-and-bins problem where y_L balls (bit errors) are thrown randomly into L bins (code blocks). Let Z_ℓ be a random variable representing the number of bit errors in the ℓ -th code block after deinterleaving. The probability of Z_ℓ given y_L is binomial distributed

$$\begin{aligned} \Pr(Z_\ell = z_\ell | Y_L = y_L) &= \begin{cases} \binom{y_L}{z_\ell} \left(\frac{1}{L}\right)^{z_\ell} \left(1 - \frac{1}{L}\right)^{y_L - z_\ell}, & \text{if } z_\ell \leq y_L, \\ 0, & \text{otherwise.} \end{cases} \end{aligned} \quad (3)$$

Combining (2) and (3), and integrating out y_L yields

$$\Pr(Z_\ell = z_\ell) = \sum_{y_L=0}^{\infty} \Pr(Z_\ell = z_\ell | Y_L = y_L) \Pr(Y_L = y_L). \quad (4)$$

For the special case when $L = 1$ (no interleaving), $\Pr(Z_\ell = z_\ell | Y_L = y_L)$ (3) is 1 if $z_\ell = y_L$, and 0 otherwise. Thus, (4) reduces to

$$\Pr(Z_\ell = \xi) = \Pr(Y_A = \xi). \quad (5)$$

To make this case consistent with [10], we adopt the same approximations. The probability of a non-decodable word is the volume under the tail of $\Pr(Y_G = y_G, Y_C = y_C)$. For a code that corrects up to τ bit errors, we approximate the tail by its largest terms $\tau + 1 \leq 2y_G + y_C \leq \tau + 3$ in [10]. Therefore, in this letter, we use $\tau + 1 \leq z_\ell \leq \tau + 3$ (from (5) and (1)).

To derive post-FEC BER for the general case of $L \geq 1$, let X_ℓ be a random variable that indicates if $\tau + 1 \leq Z_\ell \leq \tau + 3$

$$X_\ell = \begin{cases} 1, & \text{if } \tau + 1 \leq Z_\ell \leq \tau + 3, \\ 0, & \text{otherwise.} \end{cases} \quad (6)$$

The expectation of X_ℓ is $E[X_\ell] = \Pr(\tau + 1 \leq Z_\ell \leq \tau + 3)$. Let X be the sum of X_ℓ 's, $X = \sum_{\ell=1}^L X_\ell$. The expected number of code blocks having between $\tau + 1$ and $\tau + 3$ errors is $E[X] = E[\sum_{\ell=1}^L X_\ell] = \sum_{\ell=1}^L E[X_\ell] = L \cdot \Pr(\tau + 1 \leq Z_\ell \leq \tau + 3)$. The decoding algorithm is assumed to be of the bounded-distance type correcting up to τ errors and leaving the received sequence unchanged in the case of more than τ errors. As discussed in [10], we may neglect the possibility of decoding to a wrong codeword for sufficiently large τ (cf. Table I). Assuming that the average number of bit errors in a code block is $\ll \tau$, we may approximate post-FEC BER as

$$\begin{aligned} P_{\text{post}} &\approx \left(\frac{\tau + 1}{n_{B,S}} \right) \frac{E[X]}{L} \\ &= \left(\frac{\tau + 1}{n_{B,S}} \right) \Pr(\tau + 1 \leq Z_\ell \leq \tau + 3). \end{aligned} \quad (7)$$

Equation (7) is consistent with [10] when $L = 1$, i.e. [10] is a special case of (7).

From $\Pr(Y_G = y_G, Y_C = y_C)$ [10], (7), (4), and (2), we calculate the required τ and L to meet a target post-FEC BER for a chosen block length $n_{B,S}$. The combination of $n_{B,S}$ and τ specifies the BCH code, and L specifies the interleaver.

III. RESULTS AND DISCUSSION

For the system in Fig. 1, symbol rate $1/T_S = 28$ Gbaud and combined transmitter-and-LO laser linewidths $\Delta\nu_N < 100$ kHz work well with a 41-tap moving average filter for VV. As an example to illustrate the use of FEC to accommodate linewidth variations, we assume that the worst-case pre-FEC performance occurs with a linewidth of $\Delta\nu_N = 19.6$ MHz. We simulate this numerically as ‘‘poor PE pre-FEC’’ in Fig. 2. Pre-FEC BER and error statistics (described in [10]) are calculated using 10^6 bits. Simulations are modeled in VPI [11].

We examine our method in two ways. In Sec. III-A, we investigate the trade-off between L and τ . In Sec. III-B, we evaluate post-FEC BER using Monte-Carlo simulations.

A. Trade-off Between Code Overhead and Interleaver Length

This section is organized as follows: First, we derive (4) for the case when bit errors are i.i.d.. Second, we calculate (4) at ‘‘poor PE pre-FEC’’ point B in Fig. 2, for different interleaver lengths L . We compare this to the i.i.d. case. Third, for points B and C in Fig. 2, we plot the trade-off between code overhead and L . Lastly, we summarize this section.

When bit errors are i.i.d., they remain so after deinterleaving. As such, the number of bit errors in the ℓ -th block is binomial distributed

$$\Pr(Z_\ell = z_\ell) = \binom{n_{B,S}}{z_\ell} p_{\text{pre}}^{z_\ell} (1 - p_{\text{pre}})^{n_{B,S} - z_\ell}. \quad (8)$$

We now consider ‘‘poor PE’’ point B in Fig. 2. In Fig. 3, we plot (4) for different L , and compare them to the i.i.d. case. When $L = 1$, at low z_ℓ , the PDF is higher for even z_ℓ than for odd. This is because $\Pr(Y_G = y_G, Y_C = y_C)$ (shown in [10]) descends more steeply in the direction of y_C than y_G for point B. Also, $\Pr(Z_\ell = z_\ell)$ has a fatter tail than (8), so a stronger code with higher overhead is needed. As L increases,

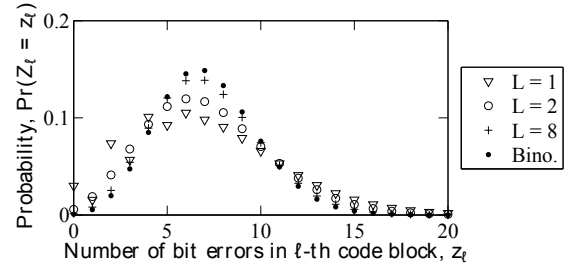


Fig. 3. $\Pr(Z_\ell = z_\ell)$ (4) at point B in Fig. 2, for code block length $n_{B,S} = 8190$ bits and different interleaver lengths L . ‘‘Bino.’’ means (8).

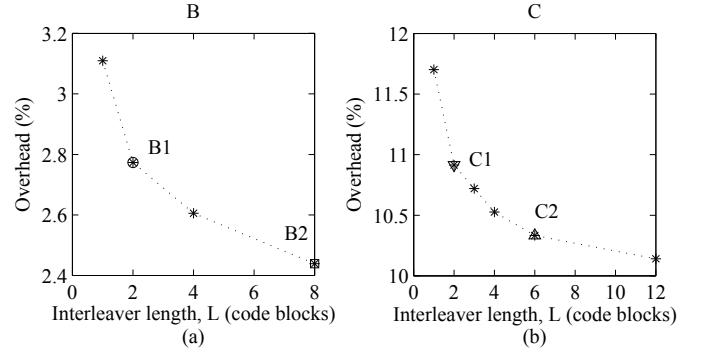


Fig. 4. Trade-off between code overhead and interleaver length L for pre-FEC points (a) B and (b) C in Fig. 2. Code block length $n_{B,S} = 8190$ bits, and overhead is $\mu\tau / (n_{B,S} - \mu\tau)$, where $\mu = \lceil \log_2(n_{B,S} + 1) \rceil$, and $\lceil x \rceil$ is the smallest integer greater than or equal to x . Interleaver-code combinations that give post-FEC BER 10^{-5} are marked with a star (*). The combinations B1, B2, C1, and C2 are listed in Table I, and used for simulations in Fig. 5.

$\Pr(Z_\ell = z_\ell)$ approaches (8), the tail becomes thinner, and a weaker code with lower overhead would suffice. This is the trade-off between code overhead and interleaver length.

Next, for ‘‘poor PE pre-FEC’’ points B and C in Fig. 2, we find combinations of τ and L that achieve a post-FEC BER target of 10^{-5} using the method in Sec. II. Code overhead vs. L is shown in Fig. 4. The greatest drop in overhead occurs when going from $L = 1$ (no interleaving) to $L = 2$. Beyond that, increasing L yields diminishing returns. Interleaving is also useful when there are only AWGN errors but no cycle slips, as AWGN error patterns have two bit errors (100% correlation). In this case, the trade-off should have the same trend as Fig. 4. However, when there are only i.i.d. cycle slips but no AWGN errors, the number of bit errors in a block is already binomial distributed, so interleaving has no effect.

To summarize, in systems with AWGN and PN, $\Pr(Z_\ell = z_\ell)$ (4) has a fatter tail than (8) when $L = 1$. As L increases, $\Pr(Z_\ell = z_\ell)$ tends to (8), i.e. its tail becomes thinner. This allows us to trade-off interleaver length with code overhead. Our method identifies the interleaver-code combinations of this trade-off (e.g. Fig. 4), thus facilitating system design based on requirements such as linewidth tolerance, implementation complexity, and processing delay.

B. Post-FEC Simulations

As an example, we aim for a target post-FEC BER of 10^{-5} using block length $n_{B,S} = 8190$ bits. We apply the

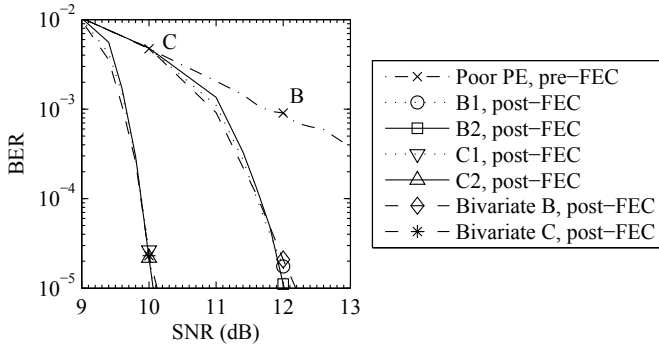


Fig. 5. BER performance. “Poor PE pre-FEC” is the same as Fig. 2. The interleaver-code combinations B1, B2, C1, and C2 used for post-FEC simulations are listed in Table I. Codes for “Bivariate B/C” are listed in [10].

TABLE I
INTERLEAVER-CODE COMBINATIONS USED FOR POST-FEC SIMULATIONS IN FIG. 5. CODE OVERHEADS ARE IN FIG. 4.

Post-FEC curve in Fig. 5	Code	τ	Overhead (%)	Interleaver length L
B1	BCH(8190,7969)	17	2.8	2
B2	BCH(8190,7995)	15	2.4	8
C1	BCH(8190,7384)	62	10.9	2
C2	BCH(8190,7423)	59	10.3	6

method in Sec. II to “poor PE pre-FEC” points B and C in Fig. 2. Possible interleaver-code combinations are shown in Fig. 4. Combinations B1 and C1 have short $L = 2$. Beyond B2 and C2, increasing L gives little improvement. We therefore simulate B1, B2, C1, and C2, as specified in Table I. Combinations B1/B2 have lower overheads than C1/C2 because B has lower pre-FEC BER than C in Fig. 2.

Post-FEC BER in Fig. 5 is calculated using 10^7 post-FEC bits, except at SNR 10 dB for C1/C2/“Bivariate C” and SNR 12 dB for B1/B2/“Bivariate B”. At those points, we simulate 10^8 post-FEC bits for better accuracy. The interleaver-code combinations designed using our method give post-FEC BERs around $2\times$ target. This performance is similar to that of codes selected using the bivariate model in [10] (Fig. 5). Furthermore, our interleaver-code combinations meet the BER target with around 0.1 dB additional SNR, which is a negligible difference in practical systems. All combinations have similar performance, i.e. our method gives consistent results. In other words, our method enables us to accurately identify combinations of binary BCH codes and interleaver lengths that achieve performance close to target.

At lower post-FEC BERs, the leading-order approximation in Sec. II and [10]—where the probability tail is approximated by its three largest terms—becomes more accurate, i.e. approximation error is less at practical post-FEC BERs of 10^{-15} than in our example with 10^{-5} . On the other hand, any inaccuracies in fitting the bivariate model $\Pr(Y_G = y_G, Y_C = y_C)$ based on pre-FEC simulations become more apparent at lower post-FEC BERs. The possibility of decoding to a wrong codeword may continue to be neglected, as this can be approximated as $1/\tau!$ [10], and τ is larger for low post-FEC BERs. As we simulate at most 10^8 post-FEC bits due to simulation limitations, the accuracy of the bivariate model has not been verified down to

post-FEC BERs of 10^{-15} . While the accuracy of our results shows that the model captures the main behavior of the system, it is possible that secondary effects involving rare events could affect accuracy at very low post-FEC BERs when interleaver length L is small. When L is large, Y_L tends to a Gaussian by the central limit theorem, so minor inaccuracies in the PDF of Y_A have little effect.

IV. CONCLUSION

In this letter, we present a semi-analytical method for designing interleavers and binary BCH codes for coherent DQPSK systems with laser PN. Our method extends [10] to systems with interleaving, and is consistent with [10]. As such, we retain the benefits of [10], including only needing short pre-FEC simulations, based on which interleaver-code combinations are designed analytically. As an example, we evaluate our approach for a 28 Gbaud system with linewidths ranging from < 100 kHz to 19.6 MHz. For a target post-FEC BER of 10^{-5} , the interleaver-code combinations identified with our method give BER around $2\times$ target, and achieve the target with around 0.1 dB extra SNR.

Future research includes assessing different interleaver implementations (e.g. pseudo- S -random interleavers), designing specifically-optimized interleavers, and investigating code/interleaver ensembles. Further refinements to improve accuracy at low post-FEC BERs may involve modeling rare events, such as more complex error patterns from VV.

ACKNOWLEDGMENT

This work was supported by Vetenskapsrådet (no. 0379801), EPSRC UNLOC EP/J017582/1, and FP7-PEOPLE-2012-IAPP (GRIFFON, no. 324391).

REFERENCES

- [1] F. Chang, K. Onohara, and T. Mizuochi, “Forward error correction for 100 G transport networks,” *Communications Magazine, IEEE*, vol. 48, no. 3, pp. S48–S55, Mar. 2010.
- [2] A. Leven and L. Schmalen, “Status and recent advances on forward error correction technologies for lightwave systems,” in *Proc. ECOC*, Sep. 2013, We.2.C.1.
- [3] S. Lin and D. J. Costello, *Error Control Coding*, 2nd ed. Prentice Hall, 2004.
- [4] A. Meiyappan, H. Kim, and P.-Y. Kam, “A low-complexity, low-cycle-slip-probability, format-independent carrier estimator with adaptive filter length,” *J. Lightw. Technol.*, vol. 31, no. 23, pp. 3806–3812, Dec. 2013.
- [5] M. Taylor, “Phase estimation methods for optical coherent detection using digital signal processing,” *Lightwave Technology, Journal of*, vol. 27, no. 7, pp. 901–914, Apr. 2009.
- [6] L. Schmalen, “Low-complexity phase slip tolerant LDPC-based FEC scheme,” in *Proc. ECOC*, Sep. 2014, Th.2.3.2.
- [7] T. Koike-Akino, K. Kojima, D. Millar, K. Parsons, Y. Miyata, W. Matsumoto, T. Sugihara, and T. Mizuochi, “Cycle slip-mitigating turbo demodulation in LDPC-coded coherent optical communications,” in *Proc. OFC*, Mar. 2014, M3A.3.
- [8] F. Yu, N. Stojanovic, F. Hauske, D. Chang, Z. Xiao, G. Bauch, D. Pflueger, C. Xie, Y. Zhao, L. Jin, Y. Li, L. Li, X. Xu, and Q. Xiong, “Soft-decision LDPC turbo decoding for DQPSK modulation in coherent optical receivers,” in *Proc. ECOC*, Sep. 2011, We.10.P1.70.
- [9] M. Y. Leong, K. J. Larsen, G. Jacobsen, S. Popov, D. Zibar, and S. Sergeyev, “Novel BCH code design for mitigation of phase noise induced cycle slips in DQPSK systems,” in *Proc. CLEO*, Jun. 2014, STu3J.6.
- [10] —, “Dimensioning BCH codes for coherent DQPSK systems with laser phase noise and cycle slips,” *J. Lightw. Technol.*, vol. 32, no. 21, pp. 3446–3450, Nov. 2014.
- [11] www.vpi-photonics.com.